Feasibility of using low-cost, byproduct materials as sorbents to remove heavy metals from aqueous solutions

Marta E. Doumer[a], Miquel Vidal[b], Antonio S. Mangrich[a], Anna Rigol[b,*],

[a]Department of Chemistry, Federal University of Paraná (UFPR), 81531-990, Curitiba, PR, Brazil

[b]Department of Chemical Engineering and Analytical Chemistry, University of Barcelona, Martí i Franquès 1-11, 08028-Barcelona, Spain

*Corresponding author: Anna Rigol; Telephone: (+34) 934039274; E-mail address: annarigol@ub.edu; ORCiD identifier: 0000-0002-3383-9684

Abstract

This work investigates the sorption of heavy metals by low-cost, byproducts such as charcoal fines (CF), waste green sand (WGS), and rice husk ash (RHA), in order to examine the feasibility of their use as alternative filter materials for metal-contaminated waters. The sorption of Cd, Cu, Pb, and Zn was investigated in batch experiments and sorption isotherms were constructed. The three byproducts showed high metal removal efficiencies (>95%, regardless of the metal concentration tested). The highest metal sorption distribution coefficients were obtained for CF, with maximum values within the 10^5-10^6 L kg^{-1} range for all the target metals. The sorption isotherms were satisfactorily fitted using the Freundlich equation and a linear model, the latter only being valid for initial metal concentrations lower than 0.4 mmol L^{-1}. Sorption reversibility was very low, with desorption yields lower than 2% and desorption distribution coefficients often higher than 10^6 L kg^{-1}. The values of the sorption and desorption parameters indicated that the use of these materials, especially charcoal fines, could constitute a low-cost alternative for the remediation of contaminated waters.

Keywords: Charcoal fines; waste green sand; rice husk ash; heavy metals; distribution coefficient.

Introduction

Aqueous effluents rich in heavy metals are produced by many industries in the metallurgical, automobile, petroleum refining, pulp and paper, and mining sectors [1]. The entry of such effluents in water bodies increases the risk of heavy metal concentrations in drinking water and groundwater exceeding regulatory thresholds, representing a challenging problem for human health and environmental management.

Various treatments can be applied to contaminated waters, although some have serious limitations. The use of ion exchange resins is expensive and requires resin regeneration, while chemical precipitation can be inefficient for low metal concentrations [2]. Hence, treatments based on the use of sorbent materials are attractive for the removal of metals present in contaminated wastewaters [2,3]. Nonetheless, materials such as activated carbon have high associated costs and are liable to loss of efficiency after regeneration processes. As an alternative, previous studies have reported the use of non-hazardous industrial and natural waste products for pollution control. For instance, metal removal by sorption onto chitosan, egg shell, potassium humate, and sugar beet lime was shown to vary in the range 60-100% for Cd, Cu, and Zn during the treatment of metal-contaminated wastewater [4]. Other wastes, such as fly ash, granular blast furnace slag, pyritic fill, and Al waste from manufacturing processes showed much higher efficiencies for the sorption of Cu from aqueous solution, compared to granular activated carbon [5].

In this work, we examine the metal sorption capacity of three materials that are receiving increasing attention for the treatment of metal-contaminated waters: rice husk ash, waste green sand, and charcoal fines. Rice husk ash (RHA) is a byproduct generated from grain processing [6] and consists mainly of amorphous silica. The low price and richness in silica of RHA has attracted much attention for its application in engineering materials, as well as in sorption processes for the removal of inorganic and organic contaminants [7]. Previous studies have revealed the potential of this material for the removal of Cd, Ni, Pb, and Zn from contaminated waters [6,8].

Waste green sand (WGS) is a solid waste generated after use of the sand to form molds for ferrous castings [9]. It consists of a blend of naturally occurring materials including silica sand (85-95%), bentonite clay (4-10%), and a carbonaceous additive (2-10%).Preliminary results have shown the efficiency of this waste material in reducing the Zn content of water when used as a sorbent in permeable reactive barriers [10], although it has not yet been tested for other heavy metals. The valorization of this waste is reduced at present, as for instance, approximately two million tons/year of WGS are sent to landfill in Brazil [11].

Charcoal fines (CF) are one of the main byproducts of the metallurgical industry, for which they are unsuitable for use because its small particle size (below 9.5 mm) causes clogging of gas passages, hence decreasing the efficiency of blast furnaces [12]. However, the use of CF as a metal sorbent can be a strategy for valorization of this waste. Preliminary studies with oxidized CF materials have indicated their high sorption capacity for V and Cu [12], but new studies are required to examine the sorption capacity of this material for other heavy metals.

In order to suggest efficient materials for the treatment of metal-contaminated waters, the present work examines the sorption of a set of metals by the WGS, CF, and RHA materials. Sorption efficiencies were evaluated in terms of the solid-liquid distribution coefficients and the rates of removal of the metals from contaminated waters. Sorption mechanisms were also proposed from the sorption data obtained using different initial metal concentrations. Finally, the sorption reversibility was also investigated in all the materials, which is supplementary information not yet considered in previous studies, especially for the CF and WGS byproducts.

Materials and Methods

Byproduct materials

The three byproducts investigated were:

- Rice husk ash (RHA), originating from the Arroz Urbano processing plant in Santa Catarina State, Brazil.

- Waste green sand (WGS), collected from the Tupy foundry in Santa Catarina State, Brazil.
- Charcoal fines (CF), originating from Irati, a Brazilian metallurgical company.

Determination of the main characteristics and structural analyses of the byproducts

The pH was measured in 1:10 (solid:water ratio) suspensions. Moisture contents were determined by drying portions of the materials at 105 ºC. The cation exchange capacity (CEC) of the CF and WGS materials were determined as described by Chapman [13], with the sorption complex saturated with Na. Due to the low CEC of RHA, it was quantified by the method described by Thomas [14], which includes a saturation step with protons. Loss on ignition (LOI) was determined by heating at 450 ºC during 4 h. Total carbon, total nitrogen, and total organic carbon (TOC) were measured by elemental analysis (EA-1108, CE Instruments, Thermo Fisher Scientific). To determine the dissolved organic carbon (DOC) content 50 mL of MiIli-Q water was added to 2 g of the material, the resulting suspension was shaken end-over-end for 30 min and the liquid phase was separated by centrifugation. The supernatant was filtered, acidified to pH 2, and the DOC concentration was determined using a total organic carbon analyzer (TOC-5000, Shimadzu).

Humic and fulvic acid contents (HA and FA, respectively) were determined in the solutions obtained by extraction at alkaline pH [15]. The total organic carbon in the extract was obtained by oxidation with potassium dichromate. An aliquot of the extract was acidified to pH 1 to precipitate the HA, which was then separated and dissolved in an alkaline medium. Finally, the total organic carbon associated with the HA fraction was determined in the resulting supernatant by oxidation of organic carbon with potassium dichromate. The FA content was calculated as the difference between the total organic carbon in the initial extract and in the HA extract.

The neutralization capacity of the samples was investigated using the CEN/TS 15364 pH titration test [16]. Firstly, the initial pH of each sample (2 g) was measured in deionized water (200 mL). The pH of the suspension was then measured after consecutive additions of 100

µL of HNO_3 or NaOH after 20 min of stirring following each addition. The acid and base addition was repeated until the range pH 2-12 was covered. The acid neutralization capacity (ANC) of the byproducts, which is an estimation of the buffering capacity with respect to external acidic stresses, was quantified form the neutralization curve as the quantity of acid or base (meq kg^{-1}) required to shift the initial pH of the sample to pH 4.

The specific surface area (SSA) of the materials was determined by N_2 adsorption measurements in liquid nitrogen, using a Micromeritics ASAP 2010 instrument. Before analysis, the samples were degassed for 2 h at 150 ºC, under vacuum.

The total contents of major and trace elements (Si, Al, Ca, Mg, Fe, Mn, K, P, As, Cd, Cr, Cu, Ni, Pb, and Zn) were determined using the modified USEPA Method 3052 [17]. 0.3 g of sample was weighed in a PTFE vessel, followed by addition of 6 mL of HNO_3 (69%), 1.5 mL of H_2O_2 (30%), and 2 mL of HF (40%). The temperature was increased to 190ºC over 15 min, followed by a dwell time of 30 min. After cooling, 16 mL of 5% H_3BO_3 was added to re-dissolve the fluoride precipitates, and the same temperature program was applied. After cooling the extracts to room temperature, they were diluted with Milli-Q water to final volumes of 50 mL and stored at 4 ºC prior to analysis by inductively coupled plasma optical emission spectrometry (ICP-OES) and inductively coupled plasma mass spectrometry (ICP-MS).

The water-soluble metal contents were quantified at a liquid/solid ratio of 25 mL g^{-1} by end-over-end shaking weighed amounts of the materials (3 g) in Milli-Q water for 16 h at room temperature. The concentrations of the elements in the extracts were subsequently determined by ICP-OES and ICP-MS.

Structural analyses were performed by X-ray diffraction (XRD), using a Shimadzu XRD-6000 instrument operated at 40 kV and 30 mA, with Ni-filtered Cu K_α radiation. Diffractograms were obtained from 10 to 80° (2θ), with a scan step of 2° min^{-1}. The XRD patterns were interpreted with the aid of Philips X'Pert HighScore software, by comparison with reference standards from the International Centre for Diffraction Data (ICDD). Diffuse reflectance

infrared Fourier transform (DRIFT) spectra of the samples were also recorded, using a Bio-Rad FTS 3500 GX spectrometer and averaging 32 scans (resolution ± 4 cm^{-1}).

Sorption and desorption tests

The sorption capacity of the materials was evaluated by batch sorption tests. Single Cd, Cu, Pb, or Zn solutions were prepared by dissolving weighed amounts of $Cd(NO_3)_2 \cdot 4H_2O$, $Cu(NO_3)_2 \cdot 3H_2O$, $Pb(NO_3)_2$, or $Zn(NO_3)_2 \cdot 4H_2O$ (Merck, Pro-Analysis) in a suitable volume of Milli-Q water to achieve a metal concentration of 100 mmol L^{-1}. 45 mL of Milli-Q water was added to material subsamples of 2 g and the resulting suspensions were end-over-end shaken for 16 h in 80-mL polypropylene tube. Suitable volumes of the corresponding metal solution were then added to have initial metal concentrations within the 0.05-5 mmol L^{-1} range (using a minimum of seven different concentrations), adjusting the final volume to 50 mL. For CF-Pb and CF-Cu, the initial metal concentration range was 1-15 mmol L^{-1}, due to the high sorption capacity of the CF material. The resulting suspensions were subsequently shaken for 24 h. The solid and liquid phases were then separated by centrifugation at 15,000 rpm for 10 min, the solutions were filtered through 0.45 µm Millipore filters, and the filtered supernatants were acidified to pH <2 with concentrated HNO_3 and kept at 4 ºC until analysis by ICP-OES and ICP-MS.

The same batch conditions were applied in parallel to control soil samples, without the presence of the metal, which allowed us to evaluate possible changes of pH and major cations (Ca and K) in the contact solutions during the heavy metal sorption process.

The byproduct residues derived from selected sorption scenarios (specifically those at 0.025, 0.10, 0.30, and 1.75 mmol L^{-1} initial metal concentrations) were dried at 105 ºC for 48 h. 50 mL of Milli-Q water were added, and the resulting suspension was end-over-end shaken for 24 h. The solid and liquid phases were separated by centrifugation at 15,000 rpm for 10 min, and the resulting solution was filtered through a 0.45 µm Millipore filter and treated as described for the sorption test.

Determination of major and trace elements in the solutions

The major and trace elements were determined in the aqueous extracts and in the solutions obtained from the sorption and desorption experiments, using a Perkin-Elmer OPTIMA 3200RL ICP-OES equipped with a Perkin-Elmer AS-90 Plus autosampler. This equipment consisted of a radiofrequency source (operating at 1150 W and a frequency of 40 MHz), a cross-flow nebulizer, and an SCD (segmented-array charge coupled device) detector. The following emission lines (nm) were used for each element determined: Cd, 214.440 and 228.802; Cr, 267.716; Cu, 324.752 and 327.393; Ni, 231.604; Pb, 220.353; Zn, 206.200 and 213.857; As, 188.979 and 193.696; Ca, 315.887 and 317.933; Mg, 279.077 and 285.213; K, 766.490; P, 178.221 and 213.617; Si, 288.158; Fe, 259.939; Al, 308.215; and Mn 259.372. The detection limits of the ICP-OES technique were: 0.01 mg L^{-1} (Cd, Cu, Fe, Mn); 0.025 mg L^{-1} (Cr, Zn); 0.05 mg L^{-1} (Al, Si); 0.1 mg L^{-1} (Ca, Mg, Ni); 0.2 mg L^{-1} (Pb); 0.5 mg L^{-1} (As, P); 1 mg L^{-1} (K).

A Perkin-Elmer ELAN 6000 inductively coupled plasma mass spectrometer (ICP-MS), equipped with a PerkinElmer AS-91 autosampler, was used for the lowest trace element concentrations. Several element isotopes (^{111}Cd, ^{112}Cd, and ^{114}Cd; ^{63}Cu and ^{65}Cu; ^{208}Pb; ^{66}Zn, ^{67}Zn, and ^{68}Zn; ^{75}As; and ^{60}Ni and ^{62}Ni) were measured to detect and control for possible isobaric or polyatomic interferences. To correct for instabilities in the ICP-MS measurements, ^{103}Rh was used in all the samples as an internal standard, at a concentration of 200 µg L^{-1}. The detection limits of the ICP-MS procedure were: 0.02 µg L^{-1} (Cd); 0.05 µg L^{-1} (Pb); 0.1 µg L^{-1} (Cu); 0.2 µg L^{-1} (As, Ni, Zn).

Data evaluation

Based on the initial metal concentration (C_i, mmol L^{-1}), the concentration in the supernatant after the sorption experiment (C_{eq}, mmol L^{-1}), and the concentration in the supernatant after the desorption experiment ($C_{eq,des,}$mmol L^{-1}), the following parameters were calculated:

a) Sorption distribution coefficient (K_d, L kg^{-1}) (Eq. 1):

$$K_d = \frac{C_{sorb}}{C_{eq}} = \frac{[(C_i - C_{eq}) \times V]/m}{C_{eq}} \quad (1)$$

where C_{sorb} (mmol kg^{-1}) is the concentration in the solid phase after the sorption experiment, V (in L) is the liquid phase volume and m (in kg) is the material weight;

b) Removal rate from solution (R, %) (Eq. 2):

$$R = \frac{(C_i - C_{eq}) \times 100}{C_i} \quad (2)$$

c) Desorption distribution coefficient ($K_{d,des}$, L kg^{-1}) (Eq. 3):

$$K_{d,des} = \frac{[(C_i - C_{eq}) \times V + C_{eq} \times V_{sol,rem} - C_{eq,des} \times V_{sol}]/m_{des}}{C_{eq,des}} \quad (3)$$

where $V_{sol,rem}$ (in L) is the volume of solution that remained in the material after the sorption test, and m_{des} (in kg) is the dry mass of material remaining in the tube after the sorption test.

d) Desorption rate (R_{des}, %) (Eq. 4):

$$R_{des} = \frac{C_{eq,des} \times V \times 100}{(C_i - C_{eq}) \times V + C_{eq} \times V_{sol,rem}} \quad (4)$$

Sorption isotherms and modeling

The experimental sorption isotherms were fitted using Freundlich and linear equations. The Freundlich sorption model describes the equilibrium on heterogeneous surfaces, without assuming monolayer coverage, and is given by:

$$C_{sorb} = K_F C_{eq}^N \quad (5)$$

where C_{eq} (mmol L^{-1}) is the concentration in the solution; C_{sorb} (mmol kg^{-1}) is the metal sorbed at equilibrium; K_F is the Freundlich constant, describing the partitioning of the solute between the solid and liquid phases; and the parameter N provides information about the

heterogeneity of the sorption sites and indicates the degree of linearity of the sorption isotherm.

Results and Discussion

Characterization of byproducts

Table 1 summarizes the main characteristics of the byproducts. The three materials showed basic pH (especially RHA) and low CEC values. A high LOI value for the CF material confirmed its high organic matter content, in agreement with its high C (%) value. On the other hand, the RHA and WGS byproducts were essentially inorganic, according to their low LOI values and low contents of TOC and C. The CF byproduct presented the highest SSA, while the value for RHA was lower than that previously reported for a similar material [8], and the SSA for WGS was similar to that reported by [9].

The ANC was low for all the samples, despite their initial alkaline pH. The values were lower than those reported for other industrial waste byproducts such as sugar foam, bentonites, fly ash, zeolites, and silicates [18]. The ANC sequence of values agreed with that of the TOC content, and their low values were also in agreement with the low CEC values and the low HA and FA contents [19].

In terms of the major elements, it can be highlighted the high total content and water-soluble fractions of K in CF (and to a lesser extent in RHA), as well as the high P content of RHA, which also presented the highest water-soluble P content of the materials tested. Finally, the Fe content was highest in CF, followed by WGS, in agreement with their origins.

The low concentrations of the water-soluble fractions of the trace elements in the materials indicated that the contribution of the original heavy metals in the sorption experiments could be considered negligible.

The DRIFT spectra of CF, RHA, and WGS are shown in Figure 1a.The peak at around 1100 cm^{-1} was more intense for the RHA and WGS byproducts, and was attributed to functional groups responsible for the CEC of the materials (Si-O-Si and -C-O-H stretching, and -OH deformation) [8]. The CF spectrum indicated the presence of a greater number of functional

groups that could play a role in metal sorption, with a prominent band at 1600 cm^{-1} that was assigned to stretching of C=C or C=O in aromatic rings [12]. A peak at 1375 cm^{-1} was due to bending of phenol -OH [20], and a peak at 1400-1420 cm^{-1} was attributed to symmetric C=O stretching.

Figure 1b shows the XRD patterns of the byproducts. CF presented an amorphous phase centered at 25°, probably associated with the amorphous structure of carbon [21]. In agreement with the DRIFT analyses, the presence of quartz impurities was noticed. The RHA material showed the presence of cristobalite (SiO_2), a quartz polymorph [8]. The main crystalline phase in WGS was quartz, with a small proportion of montmorillonite, in agreement with the use of bentonite in the preparation of the material.

Metal sorption isotherms

Description of the sorption isotherms and derived sorption parameters

Figure 2 shows the C_{sorb} vs. C_{eq} sorption isotherms for all the metal/byproduct combinations investigated. The isotherms generally followed a similar pattern, and could be classified as high-affinity (H-type) isotherms, reflecting higher affinity of the materials for the metals at low metal concentrations (C_i < 0.4 mmol L^{-1}) , with the affinity decreasing at higher initial metal concentrations [22]. The isotherms were consistent with the low DOC contents of the materials, so no effects of competitive sorption between functional groups of the solid phase and soluble organic matter were expected at low metal concentrations [23]. Isotherm pattern was also consistent with the presence of high-affinity sites for heavy metals at initial metal concentrations below 0.4 mmol L^{-1}. Thus, the presence of silicates and clay phases in RHA and WGS and the presence of organic functional groups in CF might be responsible for the formation of inner-sphere surface complexes that have strong affinity for heavy metals at low metal loadings.

Table 2 shows the minimum ($K_{d,min}$) and maximum ($K_{d,max}$) distribution coefficient values for all the metal/byproduct combinations investigated. As expected for H-type isotherms, the differences between $K_{d,max}$ and $K_{d,min}$ were of at least one order of magnitude, and for the CF

byproduct often exceeded three orders of magnitude. Considering the $K_{d,max}$ data, the CF material showed the highest affinity for the metals studied, with values within the range 10^5-10^6 L kg^{-1}, followed by RHA (for Cu, Pb, and Zn) and WGS (for Cd). The removal rates derived from $K_{d,min}$ (R_{min}) and $K_{d,max}$ (R_{max}) always exceeded 95%, confirming the efficiency of the byproducts for the treatment of metal-contaminated waters.

The K_d values obtained for the CF material were generally higher than the range of values reported in the literature for other byproducts such as chitosan, egg shell, sugar beet lime, and biochars [24,25]. For the RHA material, the K_d values obtained here were close to or higher than those reported in other studies with rice husk derived materials [6,26]. In contrast, the values obtained here for WGS were much higher than those reported, especially for Zn [10], probably due to the higher pH of the sorption experiments in the present work. The high metal affinity observed for the CF material could be explained by its high pH, its highest specific surface area among the materials tested here, and a significant presence of organic carbon, similar to that in biochars [24], and thus of surface functional groups, as observed in the DRIFT analyses. This is in agreement with previous studies that have reported the strong binding of metals such as Cu and Pb with coal-based sorbents, due to the abundance of surface functional groups including phenolic and carboxylic species [27,28].

Fitting of sorption isotherms

The experimental sorption data were first fitted using the Freundlich model. The resulting parameters (N and K_F) are given in Table 2, and Figure 2 displays the fitted curves of the sorption isotherms. The Freundlich fitting provided an excellent description of the sorption, with correlation coefficients exceeding 0.93. The values of the N parameter were lower than 1 in all cases, in agreement with the observed isotherm pattern. As C_{eq} was below 1 mmol L^{-1} in all cases, the K_F values were the result of an extrapolation to higher C_{eq} and were systematically lower than $K_{d,min}$.

Since K_F values are only fully comparable when they are associated with similar N values [29], two additional sorption parameters at the low concentration range were calculated in order to enhance comparisons among the metal/byproduct scenarios investigated. On one side, $K_{d,Freundlich}$ was calculated at C_{eq} of 0.0002 mmol L^{-1}, a metal concentration that could be of environmental relevance and is within the range of maximum metal concentration thresholds often established for drinking water (between $4x10^{-5}$ and 0.08 mmol L^{-1}, depending on the metal considered) [30]. On the other hand, $K_{d,linear}$ values were derived from the slope of the linear regressions in the region of low initial metal concentration (always lower than 0.4 mmol L^{-1}). Values of $K_{F,Freundlich}$ and $K_{d,linear}$ are also included in Table 2. An excellent correlation was obtained between the $K_{d,Freundlich}$ and $K_{d,linear}$ values (R^2 = 0.97). The $K_{d,Freundlich}$ and $K_{d,linear}$ parameters also correlated well with $K_{d,max}$ (R^2 = 0.98 and R^2 = 0.99, respectively). This indicated that both $K_{d,Freundlich}$ (calculated at a low metal concentration) and $K_{d\ linear}$ satisfactorily described the sorption capacities of the byproducts. The parameter values confirmed that the CF material had the greatest sorption capacity for the metals present at concentrations of environmental interest.

Sorption mechanisms

Changes in pH and in the concentrations of Ca, Mg, and K in the contact solutions after metal sorption were recorded in selected cases (experiments with metal C_i of 0.1, 1, and 5 mmol L^{-1}) to further understand the mechanisms of sorption of the metals by the byproducts. Results are summarized in Table 3. An increase in the initial metal concentration generally led to a decrease in the pH of the equilibrium solution, compared to the control scenario without addition of the metal. For several metal/byproduct combinations, the difference ranged from tenths of a pH unit (for the lowest metal concentration) to nearly four pH units (for the highest metal concentration, especially in the case of the RHA material).

In addition, there was a general increase in the Ca+Mg and K concentrations in the final contact solutions as the initial metal concentration increased, which could be explained by a displacement of these cations from the solid phase due to ionic exchange-based heavy metal

sorption. In contrast, changes in the Ca+Mg concentration were often minor or even negligible for initial metal concentrations of 0.1 mmol L^{-1}, especially for the RHA and WGS materials, and for Cd with CF, indicating a minor contribution of the ionic exchange process in the metal sorption, with Ca+Mg and K concentrations similar to those in the control solutions. For the WGS material with a low initial K concentration in the solution, there was no observable effect for this cation. These results were in agreement with those reported previously for other materials, indicating an increasing role of the ionic exchange when increasing the metal initial concentration [31,32]. Thus, these data supported the role of cationic exchange as the predominant sorption mechanism at high metal loadings, together with a contribution from the formation of inner-sphere surface complexes at low metal concentrations [31,33]. This was also in agreement with the presence of functional groups in the byproducts that could interact with heavy metals by means of ionic exchange mechanisms [25,31]. However, additional mechanisms cannot be discarded at high initial metal concentrations, as for initial metal concentration of 5 mmol L^{-1} the ratio between the amount of sorbed metal and the net increase in the concentrations of Ca+Mg and K released to the solution increased to values much higher than 1 for the RHA and WGS materials, suggesting the possible existence of other sorption mechanisms, such as precipitation [23,31]. In fact, previous studies have indicated that Zn precipitation could contribute its sorption by WGS [10].

Evaluation of sorption reversibility

The results of the desorption tests permitted the calculation of the desorption solid-liquid distribution coefficient ($K_{d,des}$) and the desorption yield (R_{des}) (Table 4). The $K_{d,des}$ values were systematically higher than the corresponding K_d values, exceeding 10^6 L kg^{-1} in all cases, confirming that the sorption was essentially irreversible. The minimum desorption yields ($R_{des,min}$, %) generally corresponded to the scenario in which the sorption test had been carried out with the lowest initial metal concentration, with all values below 2%, whereas the desorption yields increased up to 6% ($R_{des,max}$, %) for the scenarios derived from sorption at

the highest C_i. The low metal leaching agreed with reported values for C-based sorbents. For instance, desorption yields below 4% were obtained for a coal (oxihumolite) sorbent [27], whereas desorption yields below 5% were reported for Cd and Zn, using similar rice husk derived materials [26].

It is difficult to predict desorption data from sorption parameters. However, for all the materials, an inverse relation was generally observed between the desorption yields and the K_d values for a given metal, as illustrated in Figure 3 for Cd and Zn. An explanation is that at low concentrations the sorption occurred at specific sites, with low sorption reversibility, while at higher concentrations the metal was mainly sorbed at low-affinity sites, with higher sorption reversibility. Therefore, at low metal concentrations that are more representative of environmental scenarios, metal sorption by the byproducts studied here was characterized not only by a relatively high K_d, but also by low sorption reversibility.

Conclusions

Characterization of metal sorption and desorption using three low-cost sorbents derived from non-hazardous wastes (rice husk ash, waste green sand and charcoal fines) indicated their suitability as cost-effective materials for the removal of heavy metals from contaminated waters, providing removal rates exceeding 99.9% at low metal concentrations. Among the materials tested, the charcoal fines presented the highest metal sorption capacity, with K_d values sufficiently high that the material could even be considered as a candidate for soil remediation.

Desorption tests showed that in most cases, the heavy metals were strongly retained on the sorbents, minimizing risks of their subsequent mobilization into the environment, as high sorption K_d values were combined with low sorption reversibility.

Acknowledgements

This research was supported by the Spanish Ministerio de Economía y Competitividad (Projects CTM2011-27211 and CTM2014-55191-R) and the Generalitat de Catalunya

(AGAUR 2014SGR1277). The authors are indebted to CNPq and CAPES for a doctorate scholarship (MED) and research scholarships (JBA, ASM, AWJ, and EHN).
The authors wish to thank the Tupy foundry for supplying the green sand; the Irati metallurgical company for the coal fines; and Arroz Urbano for the rice husk ash.

References

[1] Barakat MA. New trends in removing heavy metals from industrial wastewater. Arab J Chem. 2011;4:361–377.

[2] Fu F, Wang Q. Removal of heavy metal ions from wastewaters: A review. J Environ Manage. 2011;92:407–418.

[3] Gupta VK, Ali I, Saleh TA, Nayak A, Agarwal S. Chemical treatment technologies for waste-water recycling-an overview. RSC Adv. 2012;2:6380–6388.

[4] Shaheen SM, Eissa FI, Ghanem KM, Gamal El-Din HM, Al Anany FS. Heavy metals removal from aqueous solutions and wastewaters by using various byproducts. J Environ Manage. 2013;128:514–521.

[5] Grace MA, Healy MG, Clifford E. Use of industrial by-products and natural media to adsorb nutrients, metals and organic carbon from drinking water. Sci Total Environ. 2015;518-519:491–497.

[6] Naiya TK, Bhattacharya AK, Mandal S, Das SK. The sorption of lead(II) ions on rice husk ash. J Hazard Mater. 2009;163:1254–64.

[7] Soltani N, Bahrami A, Peach-Canul MI, González LA. Review on the physicochemical treatments of rice husk for production of advanced materials. Chem Eng J. 2015;264:899–935.

[8] Srivastava VC, Mall ID, Mishra IM. Characterization of mesoporous rice husk ash (RHA) and adsorption kinetics of metal ions from aqueous solution onto RHA. J Hazard Mater. 2006;134:257–267.

[9] Lee T, Benson CH, Eykholt GR. Waste green sands as reactive media for groundwater contaminated with trichloroethylene (TCE). J Hazard Mater. 2004a;109:25–36.

[10] Lee T, Park J, Lee J-H. Waste green sands as reactive media for the removal of zinc from water. Chemosphere. 2004b;56:571–581.

[11] Ferreira GC dos S, Domingues LGF, Teixeira I, Pires MSG. Viabilidade técnica e ambiental de misturas de solo com areia descartada de fundição. Transportes. 2014;2:62–69.

[12] Angelo LC, Mangrich AS, Mantovani KM, Santos SS. Loading of VO^{2+} and Cu^{2+} to partially oxidized charcoal fines rejected from Brazilian metallurgical industry. J Soils Sediments.2013;14:353–359.

[13] Chapman HD. Cation-Exchange Capacity. American Society of Agronomy and Soil Science Society of America, Madison, 1965.

[14] Thomas GW. Methods of Soil Analysis. Chemical and Microbial Properties, 2nd ed. American Society of Agronomy and Soil Science Society of America, Madison, 1986.

[15] BOE. Real Decreto 1110/1991, de 12 de julio, por el que se aprueban los métodos oficiales de análisis de productos orgánicos fertilizantes. Boletín Oficial del Estado, 17 Julio 1991. 1991;170:23725– 23730.

[16] CEN/TS 15364. Characterisation of waste. Leaching behaviour test. Acid and basic neutralisation capacity test. European Committee of Standardization, Brussels, 2006.

[17] USEPA. United States Environmental Protection Agency, Method 3052 - Microwave assisted acid digestion of siliceous and organically based matrices. Washington, DC, 1996.

[18] González-Núñez R, Alba M, Orta M. Remediation of metal-contaminated soils with the addition of materials–Part I: Characterization and viability studies for the selection of non-hazardous waste materials. Chemosphere. 2011;85:1511–1517.

[19] Venegas A, Rigol A, Vidal M. Viability of organic wastes and biochars as amendments for the remediation of heavy metal-contaminated soils. Chemosphere. 2015;119:190–198.

[20] Qian K, Kumar A, Zhang H, Bellmer D, Huhnke R. Recent advances in utilization of biochar. Renew Sustain Energy Rev. 2015;42:1055–1064.

[21] Mopoung S. Surface image of charcoal and activated charcoal from banana peel. J Microsc Soc Thail. 2008;22:15–19.

[22] Hinz C. Description of sorption data with isotherm equations. Geoderma. 2001;99:225–243.

[23] Kołodyńska D, Wnetrzak R, Leahy JJ, Hayes MHB, Kwapiński W, Hubicki Z. Kinetic and adsorptive characterization of biochar in metal ions removal. Chem Eng J. 2012; 197:295–305.

[24] Doumer ME, Rigol A, Vidal M, Mangrich AS. Removal of Cd, Cu, Pb, and Zn from aqueous solutions by biochars. Environ Sci Pollut Res. 2016;23:2684–2692.

[25] Ding W, Dong X, Ime IM, Gao B, Ma LQ. Pyrolytic temperatures impact lead sorption mechanisms by bagasse biochars. Chemosphere. 2014;105:68–74.

[26] Srivastava V, Mall I, Mishra I. Removal of cadmium (II) and zinc (II) metal ions from binary aqueous solution by rice husk ash. Colloids Surfaces A Physicochem Eng Asp. 2008;312:172–184.

[27] Janos P, Sypecka J, Mlckovska P, Kuran P, Pilarova V. Removal of metal ions from aqueous solutions by sorption onto untreated low-rank coal (oxihumolite). Sep. Purif Technol. 2007;53:322–329.

[28] Kalmykova Y, Strömvall A-M, Steenari B-M. Adsorption of Cd, Cu, Ni, Pb and Zn on Sphagnum peat from solutions with low metal concentrations. J Hazard Mater. 2008;152:885–891.

[29] Coles CA, Yong RN. Use of equilibrium and initial metal concentrations in determining Freundlich isotherms for soils and sediments. Eng Geol. 2006;85:19–25.

[30] USEPA. United States Environmental Protection Agency, Ground Water and Drinking Water, Current Drinking Water Standards, EPA 816-F-02. Washington, DC, 2011.

[31] Mohan D, Pittman CU, Bricka M, Smith F, Yancey B, Mohammad J, Steele PH, Alexandre-Franco MF, Gómez-Serrano V, Gong H. Sorption of arsenic, cadmium, and

lead by chars produced from fast pyrolysis of wood and bark during bio-oil production. J Colloid Interface Sci. 2007;310:57–73.

[32] Sastre J, Rauret G, Vidal M. Sorption – desorption tests to assess the risk derived from metal contamination in mineral and organic soils. Environ Int. 2007;33:246–256.

[33] Fiol N, Villaescusa I, Martínez M, Miralles N, Poch J, Serarols J. Sorption of Pb(II), Ni(II), Cu(II) and Cd(II) from aqueous solution by olive stone waste. Sep Purif Technol. 2006;50:132–140.

Table 1. Main characteristics of the byproducts

Parameter		CF	RHA	WGS
pH		8.0	9.3	7.8
Moisture content (%)		5.0	0.5	1.5
CEC ($cmol_c\ kg^{-1}$)		3.0	2.5	5.0
LOI (%)		80	5.0	5.0
TOC (%)		30	2.5	1.5
DOC ($g\ kg^{-1}$)		0.6	0.7	0.7
HA (%)		0.6	<0.5	<0.5
FA (%)		3	<0.5	1.0
C (%)		35	3.0	2.0
N (%)		1	<l.q.	0.1
H (%)		3.5	0.06	0.1
ANC ($meq\ kg^{-1}$)		535	175	150
SSA ($m^2\ g^{-1}$)		20	10.5	2.5
Major and trace elements ($mg\ kg^{-1}$)				
Si	TC	37660	429140	247550
Al	TC	145	730	71130
Ca	TC	17400	5260	1290
	WS	165	45	40
Mg	TC	3910	3090	2010
	WS	85	110	60
Fe	TC	14560	660	5400
	WS	15	5	120
Mn	TC	1215	1825	80
	WS	2	23	2
K	TC	6895	12595	7720
	WS	2075	1685	47
P	TC	1115	3165	220
	WS	25	575	5
Pb	TC	15	145	10
	WS	0.01	0.01	0.08
Zn	TC	75	55	45
	WS	0.1	0.1	1.5
Cd	TC	0.5	3.5	1.0
	WS	0.001	0.005	0.050
Ni	TC	130	10	10
	WS	0.01	0.01	0.01
Cu	TC	34	10	8
	WS	0.05	0.02	0.20
As	TC	1.0	30	1.0
	WS	0.02	0.20	0.07
Cr	TC	8	10	175
	WS	<l.q.	<l.q.	<l.q.

CF – Charcoal fines, RHA – Rice husk ash, WGS – Waste green sand.
LOI – Loss on ignition, TOC – Total organic carbon, CEC – Cation exchange capacity, DOC – Dissolved organic carbon, HA – Humic acid, FA – Fulvic acid, ANC – Acid neutralization capacity.
TC – Total content; WS – water-soluble.
<l.q. – Lower than the limit of quantification.

Table 2. Sorption parameters of the byproducts tested, and fitting parameters derived from the Freundlich equation

Material	Metal	$K_{d,min}$ (L kg^{-1})	$K_{d,max}$ (L kg^{-1})	R_{min} (%)	R_{max} (%)	K_F	N	$K_{d,Freundlich}$ [1]	$K_{d,Linear}$ [2]
CF	Cd	9695	320320	99.8	99.9	680	0.39	123250	181250
	Cu	2040	648730	98.8	99.9	555	0.23	400945	456460
	Pb	8635	$>10^6$	99.7	99.9	760	0.21	633800	583225
	Zn	8290	266290	99.7	99.9	615	0.38	115475	151450
RHA	Cd	630	4850	97.7	99.5	285	0.52	16935	4970
	Cu	595	17815	96.0	99.9	270	0.51	18030	11770
	Pb	755	20930	96.8	99.9	265	0.43	34695	11590
	Zn	640	16060	96.3	99.8	290	0.54	14600	12125
WGS	Cd	570	11910	95.8	99.8	335	0.68	5145	8070
	Cu	525	6590	95.5	99.6	320	0.68	4745	6275
	Pb	1070	16195	97.4	99.8	465	0.63	10635	7320
	Zn	575	6840	95.9	99.6	320	0.64	6620	7420

CF – Charcoal fines, RHA – Rice husk ash, WGS – Waste green sand.

[1] $K_{d,Freundlich}$ was calculated at C_{eq} = 0.0002 mmol L^{-1}.

[2] $K_{d,Linear}$ was calculated for the linear region at low initial metal concentration (C_i < 0.4 mM).

Table 3. Cations release following Cd, Cu, Pb, and Zn sorption onto the byproducts, comparing control scenarios (C_i = 0) and metal C_i of 0.1, 1, and 5 mmol L^{-1}

		Control	Cd			Cu			Pb			Zn		
	C_i	0	0.1	1	5	0.1	1	5	0.1	1	5	0.1	1	5
CF	Ca+Mg	8	9	26	113	26	32	116	17	24	106	11	26	111
	K	53	61	71	89	73	76	94	63	76	98	62	72	95
	pH	8.1	7.7	7.5	7.3	7.2	7.7	6.6	7.8	7.4	7.2	7.6	7.5	7.0
RHA	Ca+Mg	6	7	8	13	8	10	15	8	7	19	8	8	12
	K	43	50	50	52	48	55	55	45	48	55	47	49	53
	pH	9.3	9.7	8.7	6.6	9.3	7.5	5.0	9.2	8.2	5.0	9.3	7.2	5.9
WGS	Ca+Mg	3	2	8	17	10	9	17	2	8	13	2	7	17
	K	1	1	1	2	2	1	2	1	2	1	1	1	2
	pH	7.8	7.1	6.1	6.8	4.1	4.9	5.0	6.6	5.8	4.9	7.3	6.3	5.9

CF – Charcoal fines, RHA – Rice husk ash, WGS – Waste green sand.

Table 4. Desorption yields (R_{des}, %) for different metal/byproduct combinations

Metal	R_{des} (%)	CF	RHA	WGS
Cd	$R_{des,min}$	0.1	0.5	1.1
	$R_{des,max}$	0.5	3.0	3.5
Cu	$R_{des,min}$	0.2	0.2	1.5
	$R_{des,max}$	0.8	1.5	3.5
Pb	$R_{des,min}$	0.1	0.1	0.1
	$R_{des,max}$	11.4	8.5	6.0
Zn	$R_{des,min}$	0.2	0.3	2.0
	$R_{des,max}$	1.0	2.5	8.0

CF – Charcoal fines, RHA – Rice husk ash, WGS – Waste green sand.

Figure captions

Figure 1. A) DRIFT spectra of CF, RHA, and WGS; B) XRD patterns of CF, RHA, and WGS. Q = quartz (PDF 83-0539), Cri = cristobalite (PDF 75-0923), M = montmorillonite 15A (PDF 29-1498). CF – Charcoal fines, RHA – Rice husk ash, WGS – Waste green sand

Figure 2. Sorption isotherms of Cd, Cu, Pb, and Zn. Red lines indicate the Freundlich fitting. CF – Charcoal fines, RHA – Rice husk ash, WGS – Waste green sand

Figure 3. Relations between desorption yields (R_{des}) and sorption distribution coefficients (K_d) for Cd and Zn. CF – Charcoal fines, RHA – Rice husk ash, WGS – Waste green sand

A)

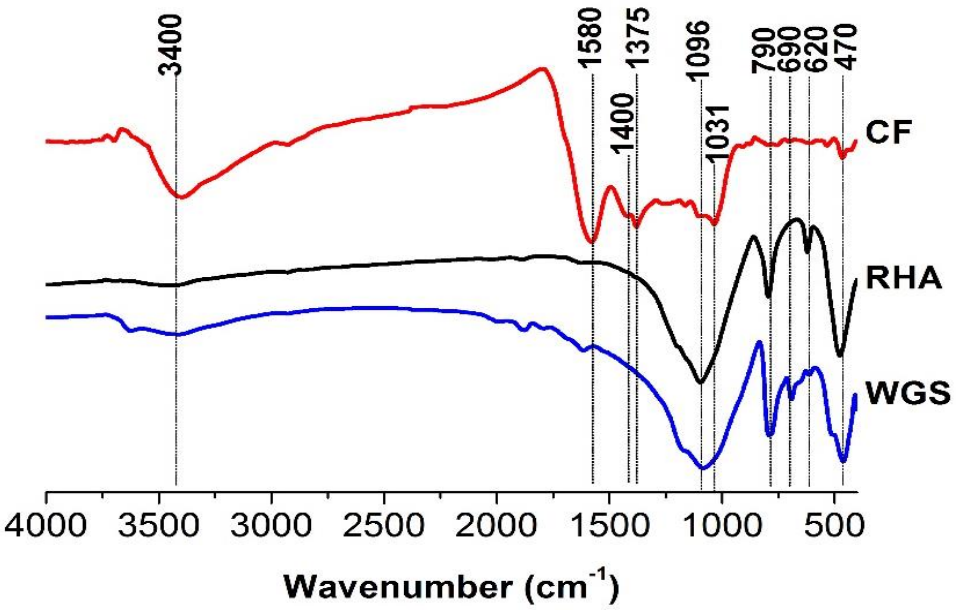
3400
1580
1375
1096
790
690
620
470
1400
1031
CF
RHA
WGS
4000 3500 3000 2500 2000 1500 1000 500
Wavenumber (cm-1)

B)

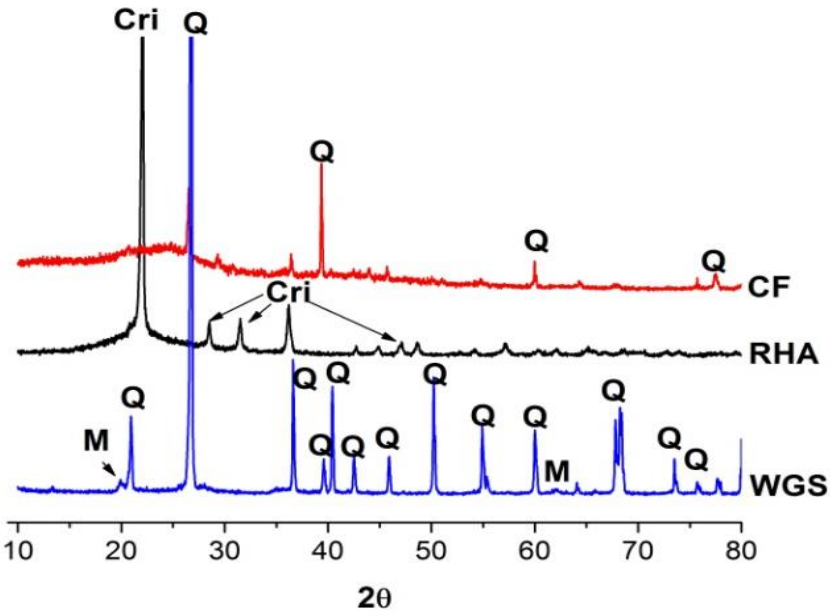
Cri
Q
Q
Q
Q
CF
Cri
RHA
Q
Q
Q
Q
Q
Q
Q
Q
M
Q
Q
Q
M
Q
Q
WGS
10 20 30 40 50 60 70 80
2θ

Fig. 1

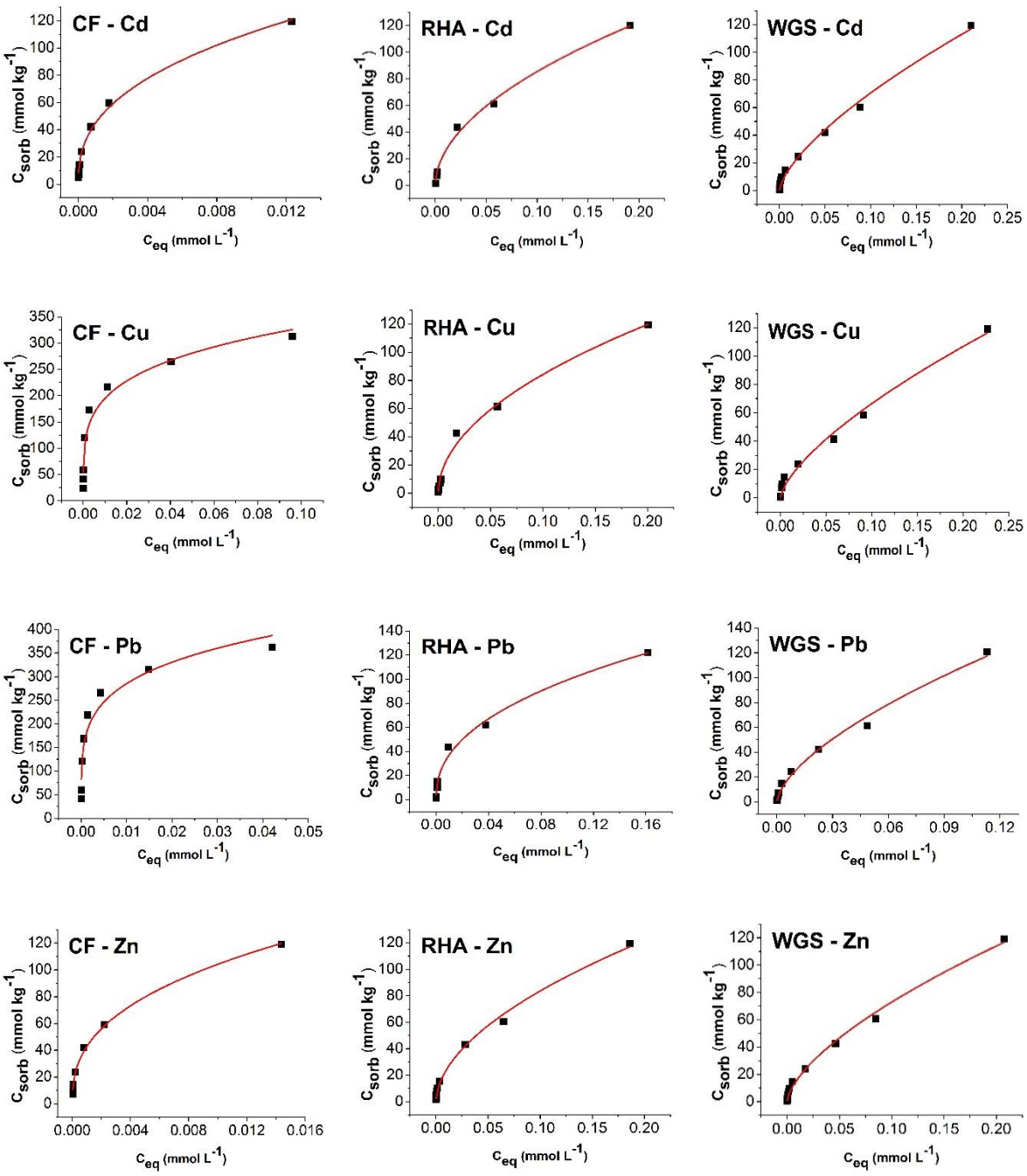
CF - Cd
RHA - Cd
WGS - Cd
CF - Cu
RHA - Cu
WGS - Cu
CF - Pb
RHA - Pb
WGS - Pb
CF - Zn
RHA - Zn
WGS - Zn
C_sorb (mmol kg^-1)
C_eq (mmol L^-1)

Fig. 2

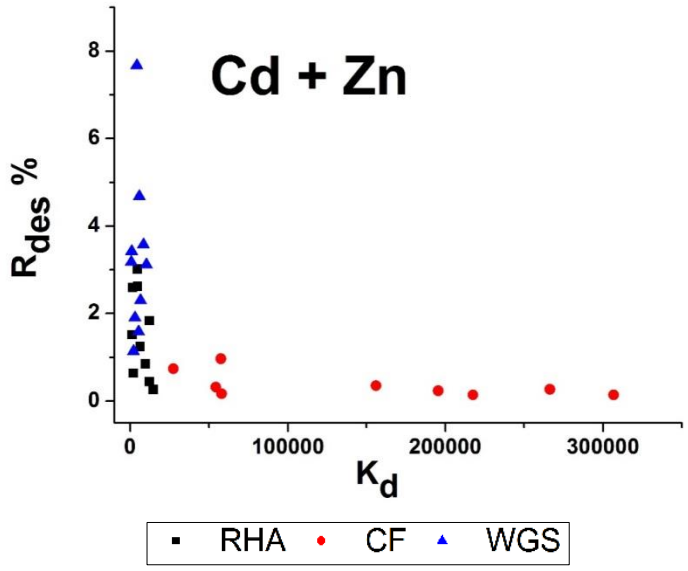

Fig. 3